Hindawi Publishing Corporation
Journal of Chemistry
Volume 2013, Article ID 605403, 13 pages
http://dx.doi.org/10.1155/2013/605403

Research Article

Host-Tailored Sensors for Leucomalachite Green Potentiometric Measurements

F. T. C. Moreira, R. B. Queirós, L. A. A. Truta, T. I. Silva, R. M. Castro, L. R. Amorim, and M. G. Sales

BioMark/ISEP and School of Engineering, Polytechnic Institute of Porto, Road Dr. António Bernardino de Almeida, 431, 4200-072 Porto, Portugal

Correspondence should be addressed to M. G. Sales; goreti.sales@gmail.com

Received 19 June 2012; Revised 8 August 2012; Accepted 8 August 2012

Academic Editor: Jose Alberto Pereira

A new biomimetic sensor for leucomalachite green host-guest interactions and potentiometric transduction is presented. The artificial host was imprinted in methacrylic acid or acrylamido-2-methyl-1-propanesulfonic acid-based polymers. Molecularly imprinted particles were dispersed in 2-nitrophenyloctyl ether and trapped in poly(vinyl chloride). The potentiometric sensors exhibited a near-*Nernstian* response in steady state evaluations, with slopes and detection limits ranging from 45.8 to 81.2 mV decade^{-1} and 0.28 to 1.01 μg mL^{-1}, respectively. They were independent from the pH of test solutions within 3 to 5. Good selectivity was observed towards drugs that may contaminate water near fish cultures, such as oxycycline, doxycycline, enrofloxacin, trimethoprim, creatinine, chloramphenicol, and dopamine. The sensors were successfully applied to field monitoring of leucomalachite green in river samples. The method offered the advantages of simplicity, accuracy, applicability to colored and turbid samples, and automation feasibility.

1. Introduction

Industrial aquaculture is a rapidly growing industry in many developed and developing countries such as Canada, Japan, Russia and China. A significant growth at food fish production has been observed over the past decade, due to the prevention or elimination of fish diseases. The introduction of veterinary medicines such as antimicrobials at the food production area has born the main responsibility for this scenario. However, the wide use of antibiotics in aquaculture led to environmental and food spread of antimicrobials and may result in the emergence of antibiotic-resistant bacteria in aquaculture environments [1, 2]. For food safety purposes, fish samples must be subject of rigorous and frequent controls that ensure that residues of antimicrobials are below the maximum legal levels [3].

Malachite green (MG) is among the drugs finding extensive use all over the world in the fish farming industry since the 1930s [4]. It is a dye and acts as a fungicide, ectoparasiticide, and disinfectant. Recent studies pointed out that it is a suspected carcinogen, showing highly cytotoxic effects to mammalian cells and acting as a liver tumor-enhancing agent. These observations lead to its restricted or prohibited use in aquaculture farming activities worldwide. Once absorbed by fish tissue, MG is metabolically reduced to leucomalachite green (LMG), its reduction product and major metabolite that is found in waters and fish tissues. Thus, an efficient and low-cost method for monitoring LMG would be highly appreciated [5], in order to prevent further dissemination of MG in the environment by means of aquaculture activities.

The analytical procedures suggested in the literature for LMG include microbiological methods [6–8] or liquid-chromatographic techniques [7–17], with fluorescence [18, 19] and/or in combination with UV, DAD, or MS detection [20–27]. The first one is unsuitable for routine control procedures, as each trial may take several days; laboratories require also proper facilities to handle biological compounds safely. Chromatographic techniques are accurate, precise, and robust, but contribute to dispose highly toxic compounds and are not sufficiently quick for routine control purposes. The same comments may apply to the electrophoretic-based

procedures reported in literature [28]. Other reported methods are based on immunoassays [29]; although they provide specific responses, the overall procedure may take a long time and turns out expensive.

Alternative and advantageous methods should rely on expeditious and efficient procedures providing highly specific and sensitive measurements. The specific recognition of a certain analyte may be achieved by molecularly imprinted polymers (MIPs). These synthetic polymers are prepared by letting functional and cross-linking monomers organize around a template (to be imprinted) and copolymerize them to form a highly cross-linked polymeric structure [30, 31]. The template is removed after creating vacant places where the functional groups of the monomeric forms are strictly oriented to bind this specific compound. The produced polymer is thus capable of rebinding the analyte with a high specificity. In many occasions it shows binding affinities approaching those presented by antigen-antibody systems [32, 33] while offering higher stability at extremes of pH and temperature, high mechanical strength, and lower cost than their natural counterparts. More recently several papers on the synthesis of MIP materials for malachite green have been published [34–37]. These materials are always obtained by bulk imprinting, being methacrylic acid (MAA) the only functional monomer tested, and applied (or intended for) chromatographic applications.

The great potential of MIP materials has led to their inclusion as recognition elements in sensors. Transduction of different nature has been employed for this purpose [38, 39], with great emphasis on electrochemisty [40]. Potentiometry is included here and offers the advantages of not requiring the template to be extracted from the membrane and the species to be diffused through the membrane [40]. Despite these advantages, most research work within this filed has been conducted only most recently [41–50].

Therefore, the present work tries to (i) develop MIP materials designed for LMG instead MG, because LMG is the major fish metabolite that may be found in waters, (ii) search for an alternative functional monomer, by replacing the traditional MAA by acrylamido-2-methyl-1-propanesulfonic acid (AMPSA), (iii) and open new horizons on the use of these materials, by applying these in biosensing development, something never done before for LMG nor MG. The sensory materials were thus synthesized with methacrylic acid (MAA) and acrylamido-2-methyl-1-propanesulfonic acid (AMPSA) functional monomers, cross-linked by ethylene glycol dimethacrylic acid (EGDMA) within the template molecule. The selective membranes were obtained by dispersing these materials in a PVC matrix, plasticized with *o*-nitrophenyl octyl ether (*o*NPOE). The potentiometric sensors were evaluated in steady-state and flowing media and applied to the analysis of contaminated water.

2. Experimental

2.1. Apparatus. All potential measurements were made by a Crison μpH 2002 decimilivoltammeter (±0.1 mV sensitivity), at room temperature, and under constant stirring, by means of a Crison, micro ST 2038. The output signal in steady state evaluations was redirected to a commutation unit linked to six ways out, enabling the simultaneous reading of six ISEs. The assembly of the potentiometric cell was as follows: conductive graphite | LMG selective membrane | buffered sample solution (phosphate, 5×10^{-2} mol L^{-1}, pH 4.5) || electrolyte solution, KCl | AgCl(s) | Ag. The reference electrode was an Orion Ag/AgCl double junction (Orion 90-02-00). The selective electrode was prepared in conventional or tubular configurations [51] for batch and flow mode evaluations, respectively. Both devices had no internal reference solution and epoxy graphite was used as solid contact.

The Flow Injection Analysis (FIA) assembly had a Gilson Minipuls 2 peristaltic pump, fitted with PVC tubing (0.80, 1.60 and/or 2.00 mm i.d.), and a four-way Rheodyne 5020 injection valve holding a loop of variable volume. The several components were gathered by PTFE tubing (Omnifit, Teflon, 0.8 mm i.d.), Gilson end-fittings, and connectors. The support devices for tubular and reference electrodes and the confluence point accessory were constructed in Perspex. After reaching a stable baseline, the emf was recorded continuously by means of a homemade high-impedance data acquisition eight-channel box connected to a PC through the interface ADC 16 (Pico Tech., UK) and PicoLog for windows (version 5.07) software.

When necessary, the pH was measured by a Crison CWL/S7 combined glass electrode connected to a decimilivoltammeter Crison, pH meter, GLP 22. A double-beam UV-vis spectrophotometer (Shimadzu model 1601) equipped with 10-mm quartz cells was used for absorbance measurements in binding studies. Infrared spectra were collected by a Nicolet 6700 FTIR spectrometer; surface measurements were carried out in ATR (attenuated total reflectance) mode with the Nicolet ATR sampling accessory of diamond contact crystal.

2.2. Reagents. All chemicals were of analytical grade and deionized water (conductivity <0.1 μS cm^{-1}) was employed. LMG, potassium *tetrakis* (4-chlorophenyl)borate (TpClPB), *o*-nitrophenyloctyl ether (*o*NPOE), poly (vinyl chloride) (PVC) of high molecular weight, EGDMA, AMPSA, and MAA were purchased from Fluka. Benzoyl peroxide (BPO), methanol (MeOH), chloroform, and tetrahydrofuran (THF) were obtained from Riedel-deHäen.

2.3. Synthesis of Host-Tailored Polymers. For molecularly imprinted polymers, the template (LMG, 1.0 mmol) was placed in a glass tube (14.0 mm i.d) with the functional monomer (4.0 mmol MAA), the cross-linker (EGDMA, 20.0 mmol), and the radical initiator (BPO, 0.24 mmol), all dissolved in 8 mL chloroform. A polymer of AMPSA was prepared similarly. The mixture was sonicated, degassed with nitrogen for 5 min, and cured at 70°C for 30 min. Nonimprinted polymers (NIP) were prepared in a similar way, by excluding the template from the procedure.

The resulting polymers were ground and sieved to particle sizes ranging from 50 to 150 μm. Extraction of the template molecule and washout of nonreacted species was carried

Table 1: Membrane composition of LMG sensors cast in 200 mg of PVC.

ISE	Active ingredient	Plasticizer	Additive	Weight (mg)
I	MIP/MAA	*o*NPOE	—	15 : 350
II	NIP/MAA	*o*NPOE	—	15 : 350
III	MIP/AMPSA	*o*NPOE	—	15 : 350
IV	NIP/AMPSA	*o*NPOE	—	15 : 350
V	MIP/MAA	*o*NPOE	TpClPB	15 : 350 : 7
VI	MIP/AMPSA	*o*NPOE	TpClPB	15 : 350 : 7
VII	MIP/MAA washed	*o*NPOE	—	15 : 350
VIII	MIP/AMPSA washed	*o*NPOE	—	15 : 350
VIII	—	*o*NPOE	—	— : 350

out with methanol/acetic acid (9 : 1, v/v). All polymers (MIP/MAA, NIP/MAA, MIP/AMPSA, and NIP/AMPSA) were let dry at ambient temperature before use.

2.4. FTIR Analysis. FTIR spectra were collected under room temperature/humidity control after background correction. The number of scans was 32 for both sample and background. x-axis was wavenumber, ranging from 525 to 4000 cm^{-1}; and y-axis was % transmittance. The resolution was 4000.

2.5. Binding Experiments. The binding studies were carried out after suitable washing of the synthesized particles. This was confirmed by measuring the absorbance of the washout solution against blank at 253 nm; the particles were repeatedly washed with methanol until LMG was no longer detected, meaning that its concentration was below the limit of detection of the spectrophotometric readings (<0.21 $\mu g\,mL^{-1}$). The polymer was let dry at ambient temperature before use.

Binding experiments were carried out by placing 20.0 mg of MIP particles (washed and dry) in contact with 10.0 mL of LMG standard solutions of varying concentrations, ranging from 0.12 to 4.0 mmol L^{-1}. The mixtures were oscillated for 12 h at room temperature and the solid phase was separated by centrifugation (3000 rpm, 10 min). The concentration of free LMG in the supernatant was calculated by UV spectrophotometry at λ_{max} = 253 nm. The increase in absorbance was directly proportional to the concentration of LMG in the supernatant, obeying Beer's law from 25 to 530 $\mu g\,mL^{-1}$.

The amount of LMG bound to the polymer was calculated by subtracting the concentration of LMG in solution (free LMG) from the initial concentration; the free LMG concentration was obtained by means of the previously indicated calibration data. The obtained data was used for Scatchard analysis.

2.6. Sensory Membranes. The sensing membranes were prepared by mixing 200 mg of PVC, 350 mg of plasticizer *o*NPOE, and 15 mg of the sensing polymer (Table 1), corresponding to a mass composition of 35.4, 61.9 and 2.7%, respectively. An amount of 7 mg of TpClPB, acting as anionic additive was added to some of these membranes; in this case, the corresponding mass composition was 35.0, 61.2, 2.6, and 1.2%, respectively. The mixture was stirred until the PVC was well moistened and dispersed in 3.0 mL THF. These membranes were placed in conductive supports of conventional or tubular shapes [51]. Membranes were let dry for 24 h and conditioned afterwards in a 1×10^{-3} mol L^{-1} LMG solution. The electrodes were also kept in this solution when not in use. The dry membranes were about 1.0 (±0.1) mm thick and got thicker after aqueous conditioning.

2.7. Potentiometric Procedures. All potentiometric measurements were carried out at room temperature. The emf values were always obtained in solutions of fixed pH/ionic strength. Increasing concentration levels of LMG was obtained by transferring 0.0200–10.0 mL aliquots of 1.0×10^{-3} mol L^{-1} LMG aqueous solutions to a 100 mL beaker containing 50.0 mL of 5.0×10^{-2} mol L^{-1} of suitable buffer. Potential readings were recorded after stabilization to ±0.2 mV. The calibration graphs plotted emf as a function of logarithm LMG concentration and were used for subsequent determination of unknown LMG concentrations.

2.8. Determination of LMG in River Water Samples. The water samples were collected from different points along *Douro* River. The collected samples had no antibiotics and were subsequently spiked with two solutions of different concentrations in LMG, in order to produce a final concentration in LMG of 50 and 100 $\mu g\,mL^{-1}$. A volume of 5.0 mL of these solutions was further diluted in 25 mL of 0.05 mol L^{-1} phosphate solution of pH 4.5. The direct potential method was applied to determine LMG in these samples.

3. Results and Discussions

The ionophore or the ion carrier is the most vital component in a polymeric membrane sensor for potentiometric transduction, in terms of selectivity and sensitivity [52]. Ion exchangers and neutral macrocyclic compounds have been employed for this purpose over the past decades. Until now, some reports found in the literature describe the use of MIP as potentiometric sensing materials. [41–50].

Noncovalent interactions between the MIP active sites and the template have been considered for allowing fast and reversible binding [52]. AMPSA and MAA were used

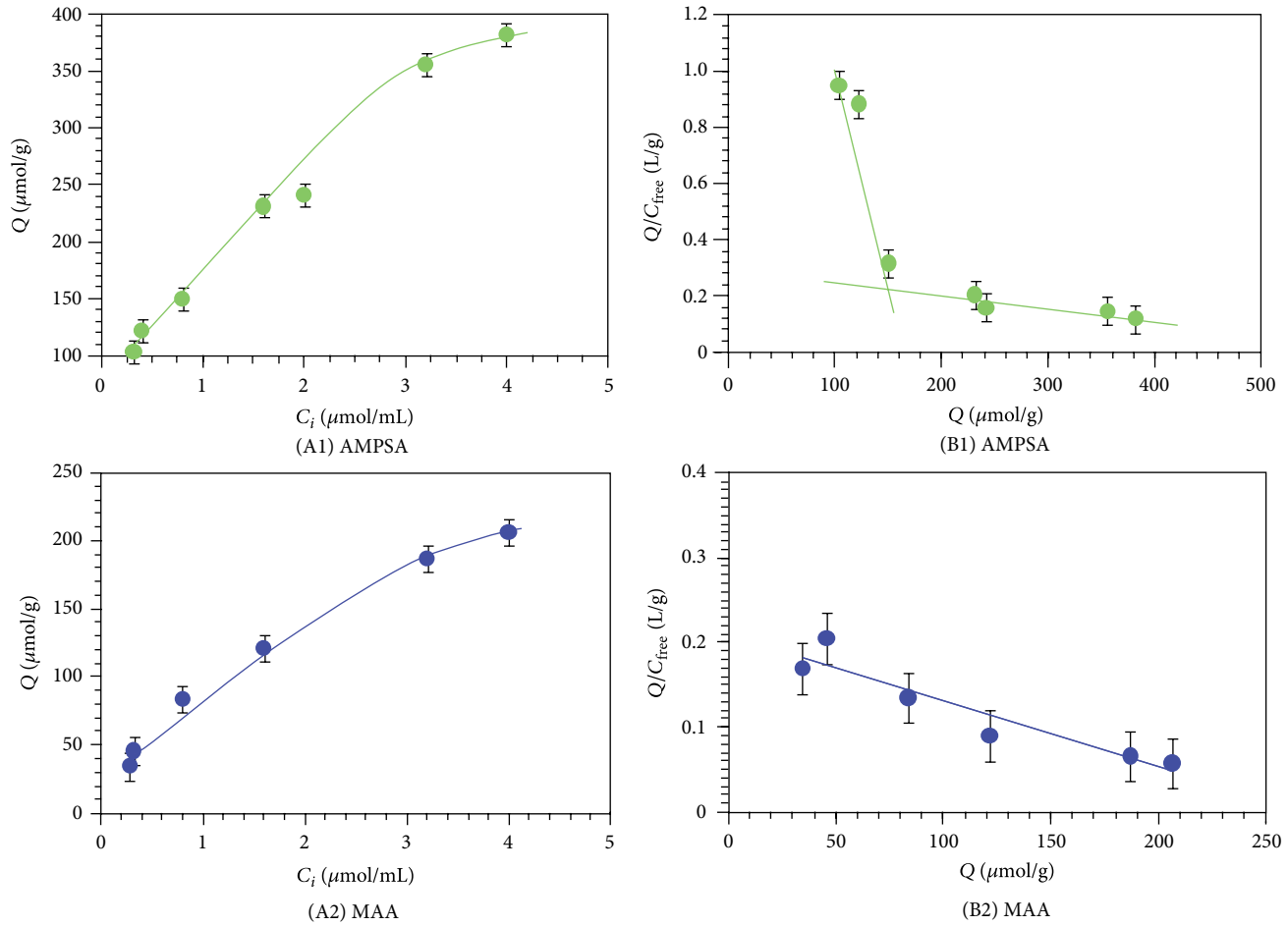

Figure 1: Binding isotherm for LMG/MAA and LMG/AAMPSO imprinted polymer Q is the amount of LMG bound to 20.0 mg of the corresponding polymer; $t = 25^{\circ}C$; $V = 10.0$ mL; binding time: 20 h. (A2) Scatchard plot to estimate the binding characteristic of LMG imprinted polymer.

as monomers as they allow electrostatic interactions mostly by hydrogen bonds with the template compound. Ion-pair interactions may also be achieved with AMPSA.

3.1. Binding Characteristic of the MIP. In liquid phase applications of MIPs, a molecule in solution interacts with binding sites in a solid adsorbent. The free ligand concentration in the liquid phase after equilibrium and reached is constant and is used to plot the corresponding adsorption isotherm.

Adsorption isotherms plot the equilibrium concentrations of bound *versus* free ligand. The bound ligand is expressed in terms of binding capacity and was calculated according to the following equation:

$$Q = \frac{\mu\text{mol (LMG bound)}}{g\,\text{(MIP)}} = \frac{(C_i - C_f)\,V_s \times 1000}{M_{\text{MIP}}}, \quad (1)$$

where Q is the binding capacity of MIPs (μmol g^{-1}), C_i the initial concentration of LMG (μmol mL^{-1}), C_f the final concentration of LMG (μmol mL^{-1}), V_s the volume of the test solution (mL), and MIP the mass of dry polymer (mg).

Thus, the synthesized particles were let stand with a wide range of LMG concentrations, for several hours and under continuous stirring. When equilibrium was reached, the free LMG concentration was calculated by UV spectrophotometry. The corresponding binding capacities were then calculated and plotted against the initial LMG concentration (Figure 1(a)). In general, the adsorption data showed that the binding capacity of the imprinted polymers increased with the increasing of the initial concentration of LMG and had a tendency to saturation for higher analyte concentrations.

The above experimental data was used to carry out the Scatchard analysis and estimate the binding parameters of MIP particles. The Scatchard equation

$$\frac{Q}{C_{\text{free}}} = \frac{(Q_{\max} - Q)}{K_d} \quad (2)$$

was applied for this purpose, where Q was the binding capacity; C_{free} the free analyte concentration in equilibrium (μmol L^{-1}); $Q_{\max}$ was the maximum apparent binding capacity; K_d was the dissociation constant of the binding site. Plotting Q/C_{free} versus Q, a liner function was expected,

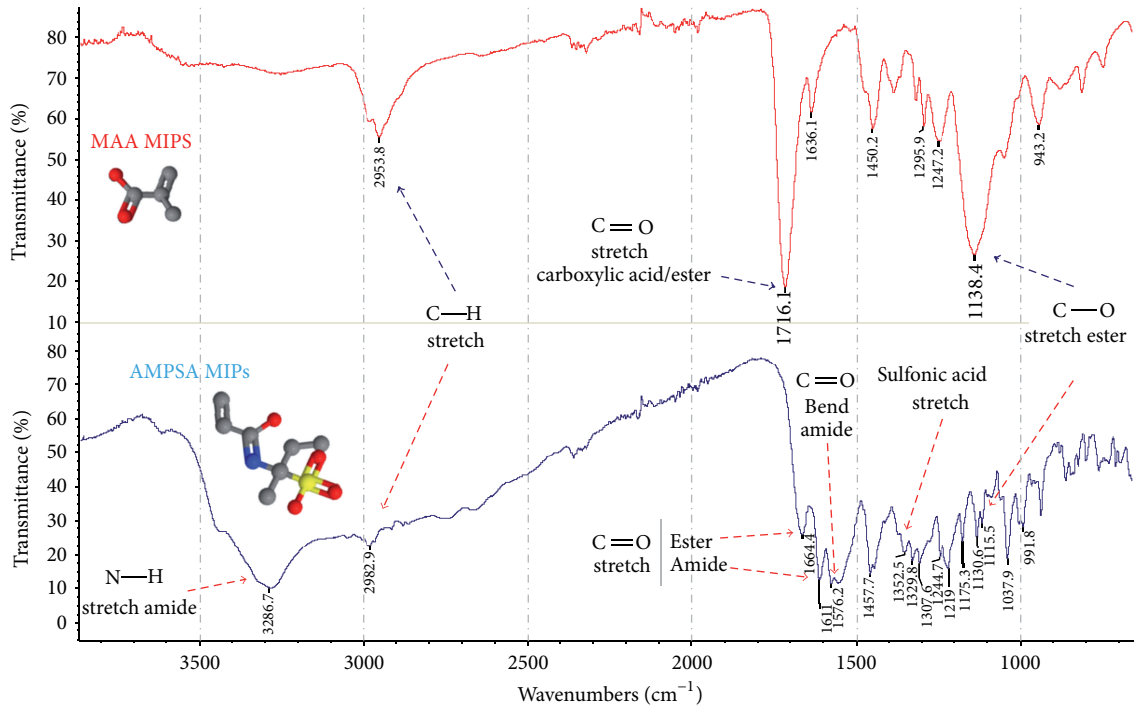

Figure 2: FITR spectra of the MAA- and AMPSA-based polymers. ATR accessory; number of scans: 32 scans; resolution: 4000.

where K_d was the slope and the y-intercept the apparent maximum number of binding sites.

The Scatchard plot for MIP particles made with AMPSA (Figure 1(B1)) showed a concave curve that is indicative of the presence of multiple classes of binding sites with different K values. Its x-asymptote behavior may also indicate the presence of nonspecific binding [53]. Overall, this concave curve suggests that the interaction of the ligand is governed by a positive cooperativity phenomenon between strong and weak binding sites [54–56]. On the contrary, the Scatchard plot of MAA MIPs displayed a linear behavior meaning that the binding sites were uniform (Figure 1(B2)) and most probably based on hydrogen-bonding interactions. The K_d and Q_{max} of the binding sites were equal to 1283 μmol L^{-1} and 268 μmol g^{-1} for dry polymer.

3.2. FTIR Data. FTIR spectra were taken by direct surface analysis of the materials, placing the MIP particles over a diamond crystal support of the ATR accessory. The resulting spectra are indicated in Figure 2. Similar spectra were observed for NIP materials because they bear the same chemical functions. The two or one peaks at about 3000–2950 cm^{-1} were assignable to absorption bands from sp^3 C–H stretching in –CH_3 and –CH_2 groups of atoms. The absence of similar bands close to these and just above 3000 cm^{-1} suggested that most monomers were suitably polymerized because no sp^2 C–H stretching was found. Absorption peaks near 1450 cm^{-1} were also attributed to sp^3 C–H bonds but resulted from bending the –CH_3 or –CH_2 groups.

The amide function in AMPSA MIPs, the carboxylic acid function in MAA MIPs, and the ester function in the cross-linker have in common a carbonyl group, making it difficult to distinguish the nature of the carbonyl involved in this strong and typical adsorption band. In general, its stretch and bend may be identified in several points of the spectra, lying within 1610–1720 cm^{-1} (Figure 2). Regarding AMPSA polymers, the amide function is clearly identified by the broad and strong adsorption band centered in 3287 cm^{-1}, corresponding to the stretch of the N–H bond. The sulfonic acid group has a typical strong adsorption at about 1350 cm^{-1}, also present in the AMPSA MIP spectrum. Regarding MAA polymers, the carboxylic acid is identifiable because of the strong and sharp adsorption band of the carbonyl group.

In general, the observed spectra confirmed the expected chemical functions, suggesting a high degree of polymerization and confirming the adequate removal of nonreacted monomers as well as template. The washout from the template was also confirmed by analyzing the MIP materials after along the several washing steps.

3.3. Sensor Performance. LMG sensors contained either MIP or NIP particles as electroactive materials dispersed in plasticized PVC. Their main analytical features were obtained under batch conditions and followed the IUPAC recommendations [57]. The results obtained are shown in Table 2. LMG sensors based in MIP particles displayed different behavior in terms of sensitivity and detection limit. The sensors prepared with MAA and AMPSA showed, respectively, linear responses starting at 5.0×10^{-5} and

Table 2: Main analytical features of the LMG potentiometric sensors in 5.0×10^{-2} mol L^{-1} phosphate buffer, pH 4.5.

ISE	Slope (mV decade^{-1})	R^2 ($n = 5$)	LOD (mol L^{-1})	LLLR (mol L^{-1})	σ_v (mV)	$C\,v_w$ (%)
I	50.7 ± 0.5	0.994	3.0×10^{-5}	5.0×10^{-5}	1.42	11
II	56 ± 5	0.996	3.2×10^{-5}	8.9×10^{-5}	3.54	3.2
III	46 ± 3	0.933	1.2×10^{-5}	1.6×10^{-5}	6.08	5.3
IV	68 ± 2	0.997	1.5×10^{-5}	3.0×10^{-5}	2.33	1.6
V	78 ± 8	0.998	4.3×10^{-5}	8.9×10^{-5}	1.77	0.95
VI	68 ± 4	0.993	1.3×10^{-5}	1.6×10^{-5}	8.16	6.0
VII	81 ± 3	0.992	3.6×10^{-5}	5.0×10^{-5}	—	—
VIII	78 ± 3	0.993	3.9×10^{-5}	5.0×10^{-5}	5.23	6.0
VIII	7 ± 3	0.972	5.3×10^{-4}	4.2×10^{-4}	5.23	1.8

Cv_w: coefficient variation if weekly calibration for 2.72×10^{-4} M; R^2: correlation coefficient; LOD: limit of detection; LLLR: lower limit of linear range; σ: standard deviation of the analytical measure for a concentration in the middle of the calibration curve, considering 3 consecutive calibrations.

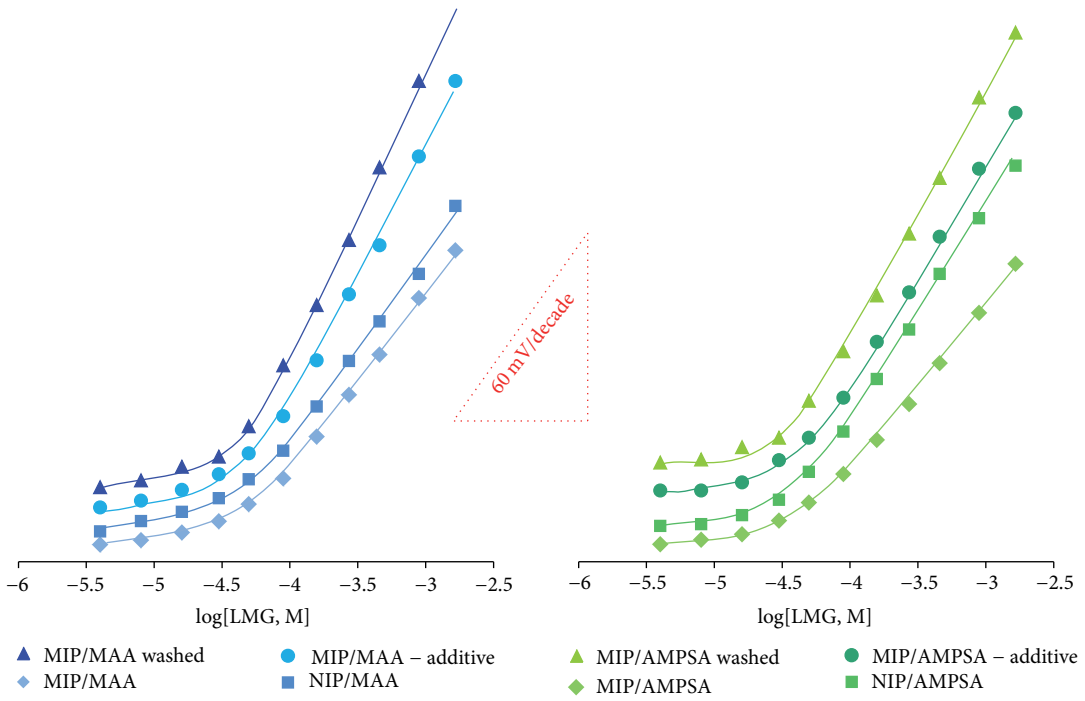

Figure 3: Potentiometric response of LMG and PVC membrane selective electrodes. Buffer: phosphate; stock solution: 5×10^{-3} mol L^{-1}, under stirring and ambient temperature.

1.6×10^{-5} mol L^{-1} LMG, cationic slopes of 50.7 and 45.8 mV decade^{-1}, and detection limits of 9.9 and 4.0 μg mL^{-1}. The corresponding NIP particles displayed a linear response after 8.9×10^{-5} mol L^{-1} and 3.0×10^{-5} LMG, cationic slopes of 55.7 and 67.7 mV decade^{-1}, and detection limits of 5.1 and 5.0 μg mL^{-1}, respectively. In general, MAA MIP sensors were the only ones presenting a near-Nernst behavior while NIP AMPSA displayed a clear super-Nernstian performance (Figure 3). Overall, the MIP sensors displayed wider linear ranges than the NIP-based sensors but this feature was coupled to the lowest slopes. This behavior may be attributed to the presence of template and unreacted monomers on the MIP materials, hindering the performance of the electrodes.

The sensors based in MIP particles were subsequently washed with methanol/acetic acid. After this procedure, they showed linear responses starting at 5.0×10^{-5} mol L^{-1} LMG, for MAA and AMPSA, respectively, cationic slopes of 81.2 and 77.8 mV decade^{-1}, and detection limits of 11.9 and 12.9 μg mL^{-1}. In general terms, super-*Nernstian* behavior was observed for both MIP sensors made with MAA and AMPSA monomers. When compared to the corresponding sensors without washing, a significant improve in terms of slope was observed for both sensors. It seems that the existence of template inside the membrane hinders the potential changes within the membrane/solution interface. This behavior could not be attributed to the mediating solvent, because a blank

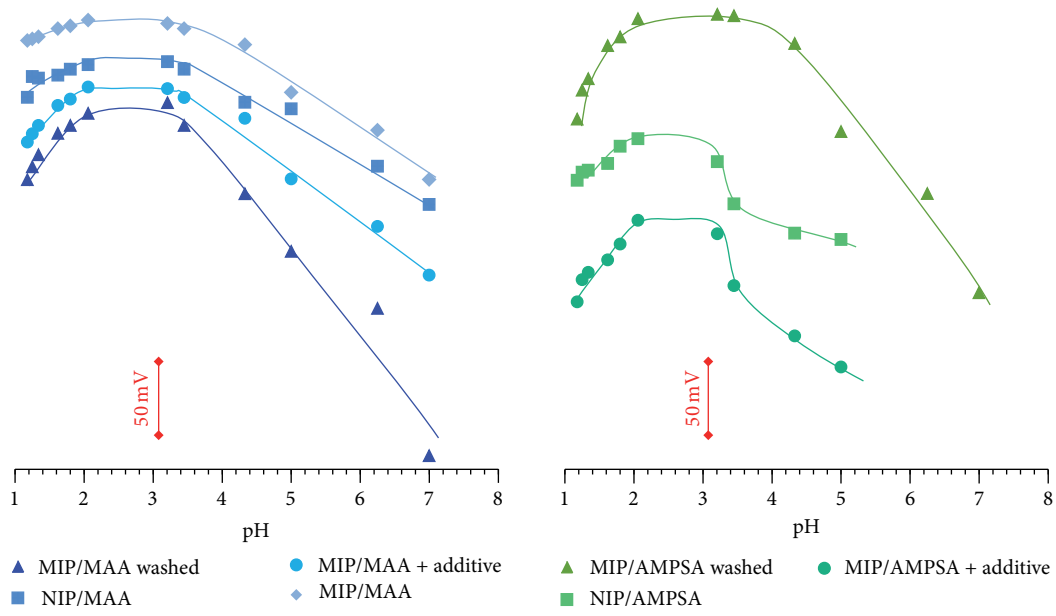

Figure 4: Reilley diagram for LMG.

membrane (without ionophore) did not respond to LMG (see Table 2).

To improve the operating features of the previous membranes, the MIP-based sensors were added of an anionic lipophilic compound. Typically, the addition of ionic compounds of lipophilic nature to potentiometric sensors reduces the anionic interference and lowers the electrical resistance of the membranes [58, 59]. In this work, TpClPB was selected for this purpose (Table 1). Sensors based in MIP/MAA and MIP/AMPSA showed linear response ranges within 8.9×10^{-5} and 1.6×10^{-5} mol L^{-1}, 14.2 and 4.3 μg mL^{-1} detection limits, and near-Nernstian responses of 78.3 and 67.9 mV $decade^{-1}$, respectively. When compared to the corresponding sensors without additive, a significant improve in terms of slope was observed for both sensors (see Figure 3).

3.4. Response Time and Lifetime. The time required to achieve a steady potential response (±3 mV) using the proposed sensors in 10^{-6} to 10^{-4} mol L^{-1} LMG solutions with a rapid 10-fold increase in concentration was <15 s. Replicate calibrations for each sensor indicated low potential drift, long-term stability, and negligible change in the response of the sensors. The sensors were stored and conditioned in 1×10^{-3} mol L^{-1} LMG solution of pH 4.5. With all sensors examined, the detection limits, response times, linear ranges, and calibration slopes were kept within ±3% of their original values over a period of at least 7 weeks.

3.5. Potential Stability and Lifetime/Reusability. The LMG sensors were stable for 1 month and were reused almost in a daily basis. The slope drifted less than 5 mV $decade^{-1}$ over this period and the linear range was unaltered. Along this period (excluding weekends), all electrodes were conditioned independently and washed with water before calibration.

The intermediate precision of the sensor was assessed by comparing three independent potentiometric measures of a specific concentration within calibrations made in different days. For a concentration of 1.4×10^{-4} mol L^{-1} in LMG solution, the average potential drift was of ±3.5 mV, thus confirming the good precision of the device. The intra-assay precision was accessed similarly by checking three consecutive calibrations and showed potential variations of ±6 mV. Overall, these results suggested a high stability of the potentiometric device.

3.6. Effect of pH. LMG has two ionizable amine groups, as may be seen in Figure 4, with a pK1 of 6.9 [60]. This feature points out the need to evaluate and control the effect of pH over the potentiometric response. This was studied for a test solution of 5.0×10^{-4} mol L^{-1} of LMG, in which pH was altered by the addition of small aliquots of concentrated hydrochloric acid or saturated sodium hydroxide solution.

The Reilley diagrams were obtained by plotting the emf of this solutions against its pH (Figure 4). The results indicated that the electrode did not respond to the pH change from 2.0 to 5.0. Lower pHs rendered an increase of the analytical signal. Since the LMG selective electrode responds to a cationic species, this increase in potential was correlated to an interference of H^+. Above pH 5.0 potentials started decreasing. This behavior was attributed to the formation of the free LMG base in the solution, leading to a decrease in the concentration of LMG ion. This was confirmed by a perceptible precipitation occurring at higher pH values. A pH of 4.5 was selected for further studies, because the

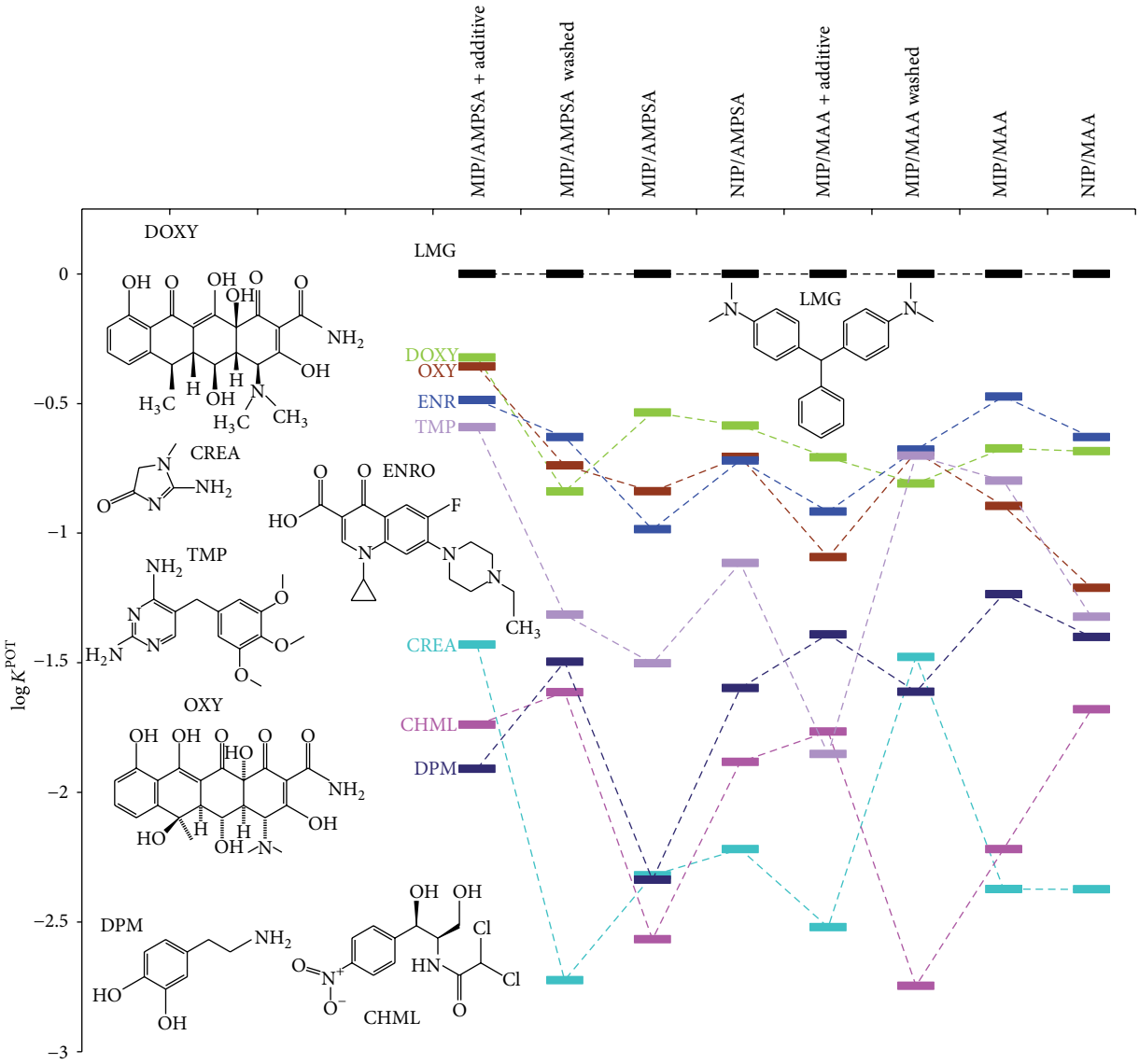

Figure 5: Potentiometric selectivity coefficients (log KPOT) of LMG membrane-based sensors. SSM solutions, in buffer, concentrations tested: 1.38×10^{-4}, 5.12×10^{-4}, and 1.02×10^{-3} mol L^{-1}, under stirring and ambient temperature.

solubility and ionization of LMG were both promoted under this condition.

3.7. Sensor Selectivity. The selectivity of the chemical sensors was evaluated by calculating potentiometric selectivity coefficients (K^{Pot}) by the separate solution method (SSM) [61]. The obtained values of $\log K^{Pot}$ were plotted in Figure 5 and indicated the degree of preferential interaction for LMG over different organic and inorganic species that are common in biological and food samples. The former group includes several antibiotics such as oxycycline (Oxy^+), doxycycline ($Doxy^+$), enrofloxacin (ENR) and trimethoprim (TMP), and creatinine ($Crea^+$), chloramphenicol (CHML), and dopamide (DPM).

The sensors with AMPSA materials showed a similar selectivity pattern. The log K^{Pot} relative order for MIP AMPSA was LMG ≫ DOXY > OXY > ENR > TMP > CREA > DPM > CHML. The corresponding washed and NIP sensors displayed similar patterns, excluding the higher interference from DPM and CHML and the lower one from DOXY. The additive on the selective membrane did not alter the general relative order of selectivity but the absolute values of log K^{Pot} were much higher. Thus, the additive deteriorated the selectivity of the MIP AMPSA-based sensor.

For the potentiometric sensors with MIP MAA-based particles the relative order of log K^{Pot} was LMG ≫ ENR > DOXY > TMP > OXY > DPM > CHML > TMP > CREA. The corresponding washed and NIP sensors displayed completely

different patterns when compared to the previous sequence. The MIP washed sensor showed the relative sequence LMG ≫ ENR ≈ TMP ≈> OXY > DOXY ≫ CREA > DPM ≫ CHML. The NIP sensor had a relative order of selectivity equal to LMG ≫ ENR > DOXY ≫ OXY > TMP > DPM > CHML ≫ CREA. Unlike in AMPSA, the additive on the MAA-based sensors improved the selectivity properties, with the exception of CHML.

In general, all sensors displayed a good selectivity for LMG, with DOXY, OXY, ENR, and TMP species interfering a bit more than DPM, CHML, and CREA. The additive on AMPSA sensors decreased the selectivity properties of the detector, for which its use in routine applications is not recommended. MG was not tested as an interfering species but it is expected to contribute significantly to the total response of the device. So, the analytical response under real conditions may be assumed as a measure of a global amount from LMG and/or MG.

3.8. Optimization of Flow Injection System. Routine analysis procedures require an expedite method. In this case, a continuous mode of operation is of regular selection and may be achieved by means FIA systems. These are particularly attractive in view of their versatility, simplicity and suitability for large-scale analyses.

The flow assembly had a double-channel, allowing the on-line adjustment of pH and ionic strength. A flow cell had a tubular configuration, as described by Kamel and coauthors [51]. It had the same graphite/epoxy conductive material as the conventional electrodes. This material filled the inner gap of a cylindrical tube (1 cm length, made of Perspex) and was machined after dry to have a 1.0 mm diameter central hole. This inner hole was coated later by the selective membrane. The resulting working electrode was of simple fabrication and allowed full membrane/sample contact, maintaining the general features of conventional configuration ISEs in terms of homogeneity, thickness, and fixed area. The reference electrode was placed after the working electrode, while the auxiliary (required to eliminate the noise created by the flowing stream) was placed before.

To take full advantages of this FIA system, flow rate and injection volume were optimized in terms of sample dilution, sensitivity, sampling rate, reagent consumption, and wastewater generation. The dispersion is amongst the most important FIA parameters to estimate the degree of sample dilution, because it depends on the capability of the electrode to reach maximum response (which relates the response time and the flow rate of the carrier). There are several ways to calculate dispersion, one of which compares the signal produced by introducing the sample as carrier (steady-state signal, H_0) or by injecting it through the loop (H). The resulting dispersion (D) for the potentiometric response is given by

$$\log D = \frac{(H_0 - H)}{S}, \tag{3}$$

where S is the slope of the flow-potentiometric system, evaluated exactly under the same experimental conditions. The percentage of steady state is another way to infer about the dilution of the sample with the carrier inside the flow tubes. It corresponds to the percentage value of H/H_0. Unlike D, it is however independent from the slope of the electrode under the underlying conditions.

The sample loop was varied within 100 and 500 μL (Figure 6). For each injection volume, a set of LMG standards ranging 1.0×10^{-4} to 1.0×10^{-2} mol L^{-1} and prepared in water was injected into the buffer carrier stream. The sensitivity of the response increased markedly with the injection volume up to 250 μL. For higher volumes the slope of the potentiometric response remained almost constant (less than 5% increase). This observation was coupled to decreased sampling rates, sample consumption, and waste generation.

The effect of flow rate was examined from 4.0 to 12.0 mL min^{-1}, recording for each condition of the above indicated calibration. No significant changes were observed in terms of slope and dispersion, but the peak width and peak height decreased with increasing flow rates. This good feature was however coupled to the production of higher amounts of wastewaters. On the other hand, for lower flow rates the sensor required long time to recover to baseline, lowering the number of sample outputs and broadening the peaks. Thus, as a compromise, a flow rate of 9 mL min^{-1} was selected for further studies.

The sensor of washed MIP/MAA was calibrated under the optimum conditions. This electrode was selected for showing the best compromise between selectivity and sensitivity. This sensor gave slopes of 45.0 mV decade^{-1} with detection limits of 10.7 μg/mL and lower limits of linear range of 1.0×10^{-5} mol L^{-1}. The sampling-rate was approximately 170 runs *per* hour.

3.9. Analytical Application. Considering the detection capabilities of the proposed device, one of its applications could be analytical sample handling prior the chromatographic analysis. Alternatively, it could be used to monitor MG applications in local farming units where its restricted use is allowed. So, the potentiometric analysis was conducted in steady state over river water. The collected samples had no antibiotics and were subsequently doped with LMG to produce contamination levels of 50 and 100 μg mL^{-1} (Table 3). These solutions were subsequently diluted 5 times with buffer to carry out the potentiometric analysis. The obtained recoveries were of 97.3 (±6.6%) or 106.5 (±0.1%), respectively, suggesting that the analytical results were accurate. The relative errors were −2.6 and +6.5%, respectively, also accounting for the good accuracy of the method. The relative standard deviation was also small, confirming the good precision of the analytical data. The t-student test confirmed that there were no significant differences between the means of the added amount and the potentiometric set of results. The calculated t-student was 0.63, below the theoretical one (12.7).

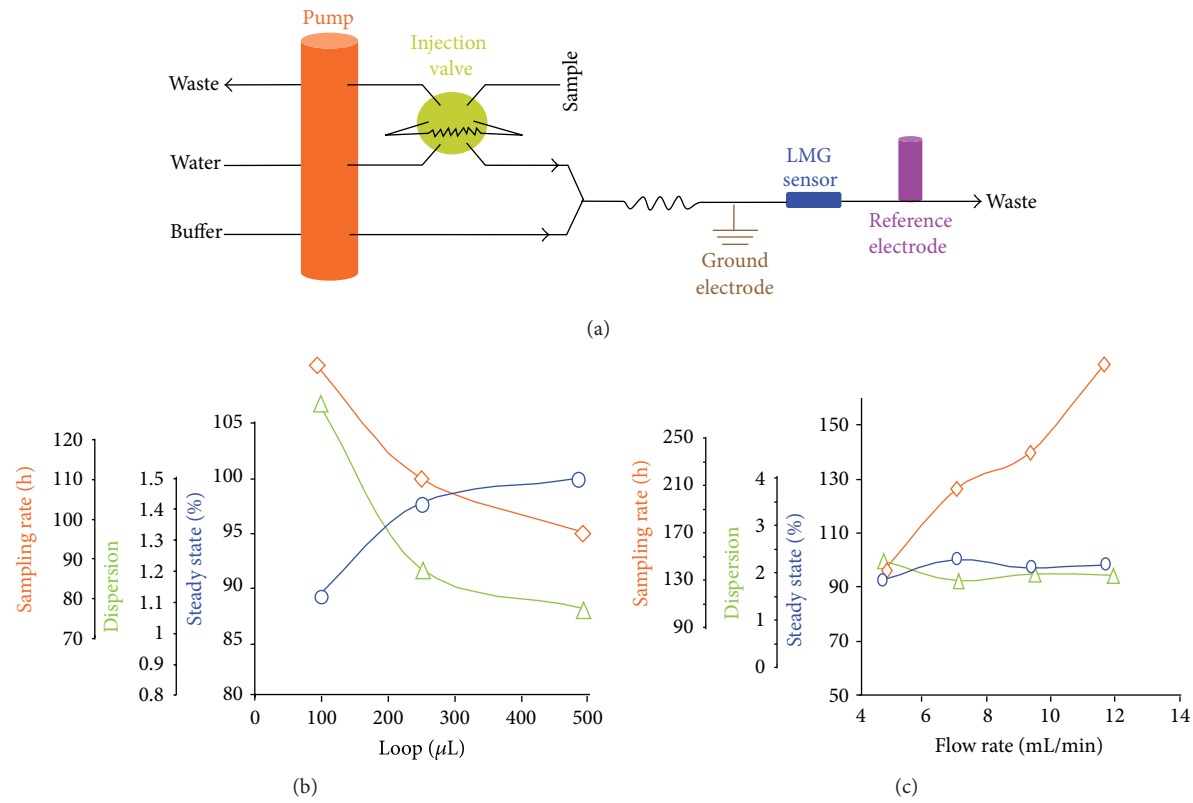

Figure 6: Double-channel FIA assembly with phosphate buffer carrier (a) and the effect of loop (b) and flow rate (c) in the dispersion, percentage steady state, and sampling rate of the reported signals. Samples/standards are prepared in water.

Table 3: Potentiometric determination of LMG in river water using MAA/MIP-based membrane sensor.

Sample	Added (μg LMG mL^{-1})	Found[(a)] (μg LMG mL^{-1})	Recovery (%)	Relative standard deviation (%)	Relative error (%)
River water 1	50	49 ± 2	97 ± 7	5.0	−2.6
River water 2	100	107 ± 1	107 ± 1	0.1	+6.5

[(a)] Found = mean ± standard deviation.

4. Conclusions

Molecular imprinting technique was employed to produce LMG host-tailored sensors for potentiometric transduction. MAA and/or AMPSA were used as monomers to produce different MIP materials. Both MAA- and AMPSA-based sensors offered good analytical features. They were capable of discriminating LMG from other amine drugs in aqueous media. The advantages of these sensors include the simplicity in designing, short measurement time, good precision, high accuracy, high analytical throughput, low limit of detection, and good selectivity.

The MIP/MAA sensors were successfully applied to the analysis of river water samples, both in steady state and in flowing media. The proposed method is simple, of low cost, precise, accurate, and inexpensive regarding reagent consumption and equipment involved. Wastewaters discharged are of small concern to environment regarding its volume and composition.

The tubular devices are particularly suitable for the routine screening control of LMG in fish food. They produce quicker responses for LMG than those provided by microbiological methods and are much less expensive than the chromatographic methods that are used for routine purposes.

Acknowledgment

The authors acknowledge the financial support from, *Fundação para a Ciência e Tecnologia* (FCT), by means of project PTDC/AGR-AAM/68359/2006.

References

[1] F. C. Cabello, "Heavy use of prophylactic antibiotics in aquaculture: a growing problem for human and animal health and for the environment," *Environmental Microbiology*, vol. 8, no. 7, pp. 1137–1144, 2006.

[2] T. Maki, I. Hirono, H. Kondo, and T. Aoki, "Drug resistance mechanism of the fish-pathogenic bacterium *Lactococcus garvieae*," *Journal of Fish Diseases*, vol. 31, no. 6, pp. 461–468, 2008.

[3] Council Regulation (EEC) 2377/90 of 26 June 1990, "Consolidated with previous amendments".

[4] S. J. Culp, F. A. Beland, R. H. Heflich et al., "Mutagenicity and carcinogenicity in relation to DNA adduct formation in rats fed leucomalachite green," *Mutation Research*, vol. 506-507, pp. 55–63, 2002.

[5] A. Swarbrick, E. J. Murby, and P. Hume, "Post-column electrochemical oxidation of leuco malachite green for the analysis of rainbow trout flesh using HPLC with absorbance detection," *Journal of Liquid Chromatography and Related Technologies*, vol. 20, no. 14, pp. 2269–2280, 1997.

[6] A. L. Henderson, T. C. Schmitt, T. M. Heinze, and C. E. Cerniglia, "Reduction of malachite green to leucomalachite green by intestinal bacteria," *Applied and Environmental Microbiology*, vol. 63, no. 10, pp. 4099–4101, 1997.

[7] J. J. Jones and J. O. Falkinham, "Decolorization of malachite green and crystal violet by waterborne pathogenic mycobacteria," *Antimicrobial Agents and Chemotherapy*, vol. 47, no. 7, pp. 2323–2326, 2003.

[8] M. C. Yang, J. M. Fang, T. F. Kuo et al., "Production of antibodies for selective detection of malachite green and the related triphenylmethane dyes in fish and fishpond water," *Journal of Agricultural and Food Chemistry*, vol. 55, no. 22, pp. 8851–8856, 2007.

[9] H. Yi, W. Qu, and W. Huang, "Electrochemical determination of malachite green using a multi-wall carbon nanotube modified glassy carbon electrode," *Microchimica Acta*, vol. 160, no. 1-2, pp. 291–296, 2008.

[10] G. Chen and S. Miao, "HPLC determination and MS confirmation of malachite green, gentian violet, and their leuco metabolite residues in channel catfish muscle," *Journal of Agriculture Food Chemistry*, vol. 58, no. 12, pp. 7109–7114, 2010.

[11] K. Halme, E. Lindfors, and K. Peltonen, "A confirmatory analysis of malachite green residues in rainbow trout with liquid chromatography-electrospray tandem mass spectrometry," *Journal of Chromatography B*, vol. 845, no. 1, pp. 74–79, 2007.

[12] W. C. Andersen, J. E. Roybal, and S. B. Turnipseed, "Liquid chromatographic determination of malachite green and leucomalachite green (LMG) residues in salmon with in situ LMG oxidation," *Journal of AOAC International*, vol. 88, no. 5, pp. 1292–1298, 2005.

[13] C. Long, Z. Mai, Y. Yang et al., "Determination of multi-residue for malachite green, gentian violet and their metabolites in aquatic products by high-performance liquid chromatography coupled with molecularly imprinted solid-phase extraction," *Journal of Chromatography A*, vol. 1216, no. 12, pp. 2275–2281, 2009.

[14] W. C. Andersen, S. B. Turnipseed, and J. E. Roybal, "Quantitative and confirmatory analyses of malachite green and leucomalachite green residues in fish and shrimp," *Journal of Agricultural and Food Chemistry*, vol. 54, no. 13, pp. 4517–4523, 2006.

[15] M. J. M. Bueno, S. Herrera, A. Uclés et al., "Determination of malachite green residues in fish using molecularly imprinted solid-phase extraction followed by liquid chromatography-linear ion trap mass spectrometry," *Analytica Chimica Acta*, vol. 665, no. 1, pp. 47–54, 2010.

[16] K. Mitrowska, A. Posyniak, and J. Zmudzki, "Determination of malachite green and leucomalachite green in carp muscle by liquid chromatography with visible and fluorescence detection," *Journal of Chromatography A*, vol. 1089, no. 1-2, pp. 187–192, 2005.

[17] K. Halme, E. Lindfors, and K. Peltonen, "Determination of malachite green residues in rainbow trout muscle with liquid chromatography and liquid chromatography coupled with tandem mass spectrometry," *Food Additives and Contaminants*, vol. 21, no. 7, pp. 641–648, 2004.

[18] K. Mitrowska, A. Posyniak, and J. Zmudzki, "Determination of malachite green and leucomalachite green residues in water using liquid chromatography with visible and fluorescence detection and confirmation by tandem mass spectrometry," *Journal of Chromatography A*, vol. 1207, no. 1-2, pp. 94–100, 2008.

[19] L. G. Rushing and E. B. Hansen, "Confirmation of malachite green, gentian violet and their leuco analogs in catfish and trout tissue by high-performance liquid chromatography utilizing electrochemistry with ultraviolet-visible diode array detection and fluorescence detection," *Journal of Chromatography B*, vol. 700, no. 1-2, pp. 223–231, 1997.

[20] H. Sun, L. Wang, X. Qin, and X. Ge, "Simultaneous determination of malachite green, enrofloxacin and ciprofloxacin in fish farming water and fish feed by liquid chromatography with solid-phase extraction," *Journal of Environmental Monitoring*, vol. 179, pp. 421–429, 2011.

[21] X. Wu, G. Zhang, Y. Wu, X. Hou, and Z. Yuan, "Simultaneous determination of malachite green, gentian violet and their leuco-metabolites in aquatic products by high-performance liquid chromatography-linear ion trap mass spectrometry," *Journal of Chromatography A*, vol. 1172, no. 2, pp. 121–126, 2007.

[22] A. Khodabakhshi and M. M. Amin, "Determination of malachite green in trout tissue and effluent water from fish farms," *International Journal of Environmental Health Engineering*, vol. 1, pp. 51–56, 2012.

[23] K. C. Lee, J. L. Wu, and Z. Cai, "Determination of malachite green and leucomalachite green in edible goldfish muscle by liquid chromatography-ion trap mass spectrometry," *Journal of Chromatography B*, vol. 843, no. 2, pp. 247–251, 2006.

[24] X. Hu, K. Jiao, W. Sun, and J. Y. You, "Electrochemical and spectroscopic studies on the interaction of malachite green with DNA and its application," *Electroanalysis*, vol. 18, no. 6, pp. 613–620, 2006.

[25] Z. Hall, C. Hopley, and G. O'Connor, "High accuracy determination of malachite green and leucomalachite green in salmon tissue by exact matching isotope dilution mass spectrometry," *Journal of Chromatography B*, vol. 874, no. 1-2, pp. 95–100, 2008.

[26] J. A. Tarbin, K. A. Barnes, J. Bygrave, and W. H. H. Farrington, "Screening and confirmation of triphenylmethane dyes and their leuco metabolites in trout muscle using HPLC-vis and ESP-LC-MS," *Analyst*, vol. 123, no. 12, pp. 2567–2571, 1998.

[27] S. B. Turnipseed, W. C. Andersen, and J. E. Roybal, "Determination and confirmation of malachite green and leucomalachite green residues in salmon using liquid chromatography/mass spectrometry with no-discharge atmospheric pressure chemical ionization," *Journal of AOAC International*, vol. 88, no. 5, pp. 1312–1317, 2005.

[28] C. H. Tsai, J. D. Lin, and C. H. Lin, "Optimization of the separation of malachite green in water by capillary electrophoresis Raman spectroscopy (CE-RS) based on the stacking and sweeping modes," *Talanta*, vol. 72, no. 2, pp. 368–372, 2007.

[29] US Patent Application 20070072242, "Immunoassay method and kit to leucomalachite green and malachite green,"

http://www.patentstorm.us/applications/20070072242/description.html.

[30] P. Spégel, L. Schweitz, and S. Nilsson, "Molecularly imprinted polymers," *Analytical and Bioanalytical Chemistry*, vol. 372, no. 1, pp. 37–38, 2002.

[31] L. I. Andersson, "Molecular imprinting for drug bioanalysis: a review on the application of imprinted polymers to solid-phase extraction and binding assay," *Journal of Chromatography B*, vol. 739, no. 1, pp. 163–173, 2000.

[32] L. Ye and K. Haupt, "Molecularly imprinted polymers as antibody and receptor mimics for assays, sensors and drug discovery," *Analytical and Bioanalytical Chemistry*, vol. 378, no. 8, pp. 1887–1897, 2004.

[33] G. Vlatakis, L. I. Andersson, R. Muller, and K. Mosbach, "Drug assay using antibody mimics made by molecular imprinting," *Nature*, vol. 361, no. 6413, pp. 645–647, 1993.

[34] Y. H. Li, T. Yang, X. L. Qi, Y. W. Qiao, and A. P. Deng, "Development of a group selective molecularly imprinted polymers based solid phase extraction of malachite green from fish water and fish feed samples," *Analytica Chimica Acta*, vol. 624, no. 2, pp. 317–325, 2008.

[35] H. Cao, F. Xu, D. X. Li, X.-G. Zhang, and J.-S. Yu, "Preparation and performance valuation of high selective molecularly imprinted polymers for malachite green," *Research on Chemical Intermediates*. In press.

[36] S. Yan, Z. Gao, Y. Fang, Y. Cheng, H. Zhou, and H. Wang, "Characterization and quality assessment of binding properties of malachite green molecularly imprinted polymers prepared by precipitation polymerization in acetonitrile," *Dyes and Pigments*, vol. 74, no. 3, pp. 572–577, 2007.

[37] C. M. Lok and R. Son, "Application of molecularly imprinted polymers in food sample analysis—a perspective," *International Food Research Journal*, vol. 16, pp. 127–140, 2009.

[38] K. Haupt and K. Mosbach, "Molecularly imprinted polymers and their use in biomimetic sensors," *Chemical Reviews*, vol. 100, no. 7, pp. 2495–2504, 2000.

[39] F. T. C. Moreira, V. A. P. Freitas, and M. G. F. Sales, "Biomimetic norfloxacin sensors made of molecularly-imprinted materials for potentiometric transduction," *Microchimica Acta*, vol. 172, no. 1, pp. 15–23, 2011.

[40] M. C. Blanco-López, M. J. Lobo-Castañón, A. J. Miranda-Ordieres, and P. Tuñón-Blanco, "Electrochemical sensors based on molecularly imprinted polymers," *Trends in Analytical Chemistry*, vol. 23, no. 1, pp. 36–48, 2004.

[41] M. Javanbakht, S. E. Fard, A. Mohammadi et al., "Molecularly imprinted polymer based potentiometric sensor for the determination of hydroxyzine in tablets and biological fluids," *Analytica Chimica Acta*, vol. 612, no. 1, pp. 65–74, 2008.

[42] L. Codognoto, E. Winter, K. M. Doretto, G. B. Monteiro, and S. Rath, "Electroanalytical performance of self-assembled monolayer gold electrode for chloramphenicol determination," *Microchimica Acta*, vol. 169, no. 3, pp. 345–351, 2010.

[43] R. Shoji, T. Takeuchi, and I. Kubo, "Atrazine sensor based on molecularly imprinted polymer-modified gold electrode," *Analytical Chemistry*, vol. 75, no. 18, pp. 4882–4886, 2003.

[44] T. Kitade, K. Kitamura, T. Konishi et al., "Potentiometric immunosensor using artificial antibody based on molecularly imprinted polymers," *Analytical Chemistry*, vol. 76, no. 22, pp. 6802–6807, 2004.

[45] G. D'Agostino, G. Alberti, R. Biesuz, and M. Pesavento, "Potentiometric sensor for atrazine based on a molecular imprinted membrane," *Biosensors and Bioelectronics*, vol. 22, no. 1, pp. 145–152, 2006.

[46] A. Warsinke and B. Nagel, "Towards separation-free electrochemical affinity sensors by using antibodies, aptamers, and molecularly imprinted polymers—a review," *Analytical Letters*, vol. 39, no. 13, pp. 2507–2556, 2006.

[47] F. T. C. Moreira, A. H. Kamel, J. R. L. Guerreiro, and M. G. F. Sales, "Man-tailored biomimetic sensor of molecularly imprinted materials for the potentiometric measurement of oxytetracycline," *Biosensors and Bioelectronics*, vol. 26, no. 2, pp. 566–574, 2010.

[48] K. P. Prathish, K. Prasad, T. P. Rao, and M. V. S. Suryanarayana, "Molecularly imprinted polymer-based potentiometric sensor for degradation product of chemical warfare agents. Part I. Methylphosphonic acid," *Talanta*, vol. 71, no. 5, pp. 1976–1980, 2007.

[49] J. R. L. Guerreiro, V. Freitas, and M. G. F. Sales, "New sensing materials of molecularly-imprinted polymers for the selective recognition of Chlortetracycline," *Microchemical Journal*, vol. 97, no. 2, pp. 173–181, 2011.

[50] A. H. Kamel, F. T. C. Moreira, S. A. A. Almeida, and M. G. F. Sales, "Novel potentiometric sensors of molecular imprinted polymers for specific binding of chlormequat," *Electroanalysis*, vol. 20, no. 2, pp. 194–202, 2008.

[51] A. H. Kamel, S. A. A. Almeida, M. G. F. Sales, and F. T. C. Moreira, "Sulfadiazine-potentiometric sensors for flow and batch determinations of sulfadiazine in drugs and biological fluids," *Analytical Sciences*, vol. 25, no. 3, pp. 365–371, 2009.

[52] F. Faridbod, M. R. Ganjali, R. Dinarvand, and P. Norouzi, "Developments in the field of conducting and non-conducting polymer based potentiometric membrane sensors for ions over the past decade," *Sensors*, vol. 8, no. 4, pp. 2331–2412, 2008.

[53] J. A. García-Calzón and M. E. Díaz-García, "Characterization of binding sites in molecularly imprinted polymers," *Sensors and Actuators B*, vol. 123, no. 2, pp. 1180–1194, 2007.

[54] F. Gritti and G. Guiochon, "Heterogeneity of the surface energy on unused C18-Chromolith adsorbents in reversed-phase liquid chromatography," *Journal of Chromatography A*, vol. 1028, no. 1, pp. 105–119, 2004.

[55] S. Sharma and G. P. Agarwal, "Interactions of proteins with immobilized metal ions: role of ionic strength and pH," *Journal of Colloid and Interface Science*, vol. 243, no. 1, pp. 61–72, 2001.

[56] C. Hidayat, M. Nakajima, M. Takagi, and T. Yoshida, "Multivalent binding interaction of alcohol dehydrogenase on dye-metal affinity matrix," *Journal of Bioscience and Bioengineering*, vol. 96, no. 2, pp. 168–173, 2003.

[57] Y. Umezawa, P. Bühlmann, K. Umezawa, K. Tohda, and S. Amemiya, "Potentiometric selectivity coefficients of ion-selective electrodes part I. Inorganic cations—(technical report)," *Pure and Applied Chemistry*, vol. 72, no. 10, pp. 1851–2082, 2000.

[58] M. Telting-Diaz and E. Bakker, "Effect of lipophilic ion-exchanger leaching on the detection limit of carrier-based ion-selective electrodes," *Analytical Chemistry*, vol. 73, no. 22, pp. 5582–5589, 2001.

[59] M. Lizondo, M. Pons, M. Gallardo, and J. Estelrich, "Physicochemical properties of enrofloxacin," *Journal of Pharmaceutical and Biomedical Analysis*, vol. 15, no. 12, pp. 1845–1849, 1997.

[60] F. L. Dickert and O. Hayden, "Molecular imprinting in chemical sensing," *Trends in Analytical Chemistry*, vol. 18, no. 3, pp. 192–199, 1999.

[61] Y. Umezawa, K. Umezawa, and H. Sato, "Selectivity coefficients for ion-selective electrodes—recommended methods for reporting $K^{\text{pot}}_{A,B}$ values—(technical report)," *Pure and Applied Chemistry*, vol. 67, no. 3, pp. 507–518, 1995.